RSC Advances

ROYAL SOCIETY OF CHEMISTRY

www.rsc.org/advances

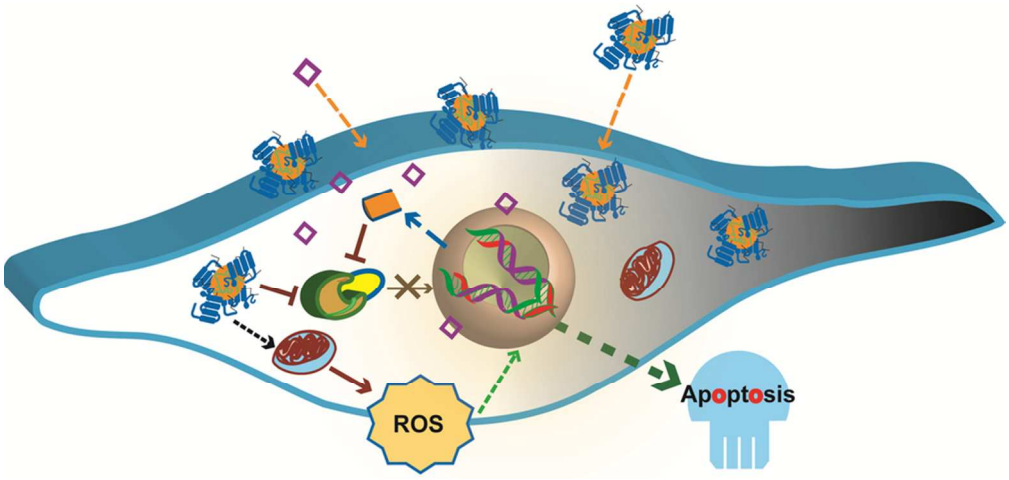

Mode of action of 5-FU and curcumin nano-conjugate on U87-IκBα cells.
85x40mm (300 x 300 DPI)

Cite this: DOI: 10.1039/c0xx00000x

www.rsc.org/xxxxxx

ARTICLE TYPE

Chemosensitization of IκBα overexpressing glioblastoma towards anti-cancer agents

Subhamoy Banerjee,[a] Amaresh Kumar Sahoo,[b] Arun Chattopadhyay[b, c] and Siddhartha Sankar Ghosh*[a, b]

Received (in XXX, XXX) Xth XXXXXXXXX 20XX, Accepted Xth XXXXXXXXX 20XX
DOI: 10.1039/b000000x

Burgeoning research on gene-directed therapeutics has significant translational scope to combat multidrug resistant glioblastoma, where conventional anticancer drugs cease to work alone or in combination. In the present work, a novel strategy to sensitize drug resistant glioblastoma cells (U87MG) has been proposed by overexpressing IκBα gene, which is a cellular inhibitor of NFκB signaling pathways. The IκBα overexpressing U87MG cell line (U87-IκBα) was established by G418 selection of IκBα transfected U87MG cells. Expression of IκBα was studied by semi-quantitative RT PCR, real time PCR and Western blot analysis. Those stable cells were found to be easily sensitized with anticancer drug, 5-fluorouracil (5-FU) and non-conventional therapeutic agent curcumin nanoparticles. Cell viability assay and flow cytometry based cell cycle studies showed dose dependent differential effects of 5-FU on U87-IκBα and U87MG cells. Expression status of various cell cycle genes were examined by the real time PCR analysis. Furthermore, water soluble curcumin nanoparticles (NPs) were synthesized in presence of poly L-Lysine and BSA to sensitize U87-IκBα cells. Results demonstrated the augmentation of therapeutic potential of 5-FU and curcumin nanoparticles on IκBα overexpressed cells. Thus, this simple strategy offers the scope of using combination module as a potential cancer therapeutic.

Keywords: U87MG, IκBα, curcumin nanoparticles, 5-fluorouracil

1. INTRODUCTION

Multiple drug resistance property of glioblastoma (brain cancer, e.g. U87MG cells) confers aggressive proliferation and differentiation along with the ability to evade the apoptotic pathway of cell death, resulting in poor response to conventional chemotherapeutics[1, 4]. This demands novel therapeutics and/or strategies to prevail the challenges of poor prognosis and huge mortality rate[2, 3]. To overcome this challenge detailed understanding of molecular events such as gene expression and regulation by various endogenous inhibitors would be a viable option as cellular events occurring with a high degree of precision govern the gene expression. This provides ample opportunity to monitor them in a better way of developing by suitable strategies in order to cure several diseases including glioblastoma. For example, in U87MG cell line several anti-apoptotic and pro-survival gene (e.g. - bcl-2, bcl-xL, survivin etc.) expression relies on NFκB which is an inducible transcription factor [5, 6]. The NFκB comprises of with five different subunits. They act as transcription factors in homo- or hetero dimeric fashion and bind to the κB binding site in the promoter region of target genes[7-9]. IκBα binds with p50/p65 heterodimer (most abundant among all the NFκB dimers) in the cytoplasm and blocks its translocation into the nucleus[10-12]. Upon induction by external stimuli (e.g.- TNF-α, LPS etc.), IKK-β phosphorylates IκBα, leading to its proteasome mediated degradation. The unbound NFκB translocates into the nucleus and initiates transcription[7-9, 11, 13]. Thus, it may be inferred that inhibition of NFκB would be a specific target in cancer chemotherapeutics. However, literature suggests that there are not many reports available to address this issue [11, 15-17]. Another crucial point is the use of small molecules like proteasome inhibitor or immunosuppressive agents which quite often exhibit several side effects [18]. Hence, there lies the scope of using naturally occurring bioactive molecules to replace these small molecules which eventually reduces the possibility of side effects after following exposure. Curcumin (diferuloylmethane) is one of the naturally occurring bioactive molecules that have been used as a model chemosensitizing agent to kill cancer cells including U87MG [19-21]. As a potent anticancer agent, curcumin is found to regulate various transcription factors, growth factors and cytokines required for the proliferation of cancer cells[22, 23]. The role of curcumin upon inhibition of pro-inflammatory transcription factor NFκB is well studied. It has been found that curcumin inhibits constitutive activation of NFκB by blocking G1/S phase of cell cycle [24-26], which in turn induces apoptosis. Also, inhibition of NFκB increases the half-life of IκBα and modulates inhibition of cell proliferation [27, 28]. It is worth mentioning that due to its poor water solubility curcumin lacks the bioavailability and biodistribution [29] which eventually limits its therapeutic index. These inherent demerits could be resolved by synthesizing curcumin NPs with a suitable surface

stabilizing agent to heighten its therapeutic potential [30, 31]. Glioblastoma cells (U87MG) are resistant to common anticancer drugs like 5-Fluorouracil (5-FU) [32, 33]. Various reports suggest that gene therapy or RNA interference increases efficacy of chemosensitization in glioma cells lines [34-36]. Overexpression of gene of interest inside the glioma cells and its sensitization with conventional anticancer agent is always advantageous over novel therapeutics as the molecular pathway of the drug activation is known. Furthermore, different reports suggest that the over expression of IκBα (and its different forms) sensitizes cancer cells towards common chemotherapeutics and radiation therapy [37-39]. Thus as a proof of concept, we have constructed wild type IκBα overexpressing U87MG cell line (hence we name it U87-IκBα) and tested the efficacy of 5-FU and curcumin NPs separately as well as in combination. Therefore, using this approach of eliciting the drug activity with the help of endogenous control, particularly to kill the drug resistant cancer cell lines, will pave a new approach for cancer therapy.

Herein, the IκBα overexpressing U87MG cell line (U87-IκBα) was established and the effect of curcumin nano-conjugate and 5-FU was studied. To synthesize water soluble curcumin NPs, biodegradable polymer poly vinyl pyrrolidone (PVP) was employed as stabilizing agents, which was further loaded with nontoxic protein BSA via poly-L-lysine to increase stability in cellular environment. This curcumin nano-conjugate was added to the U87-IκBα cells for higher therapeutic efficacy. Also, 5-FU was added to the transfected cells to study the heightened therapeutic efficacy. The layout of the work is mentioned in scheme 1.

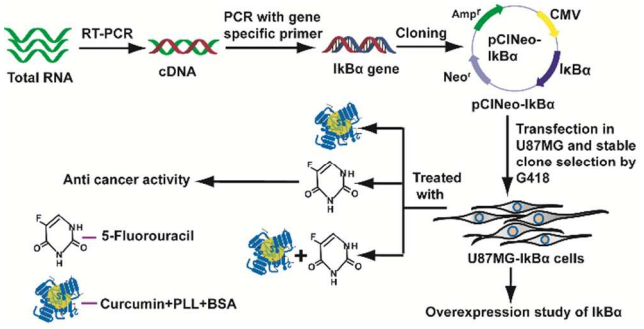

Scheme 1 Schematic of generation of U87-IκBα cell line and sensitization with 5-FU and curcumin nano-conjugate.

2. MATERIALS AND METHODS

2.1 Cloning of IκBα in mammalian expression vector

IκBα was cloned in pGEM-T Easy vector (Promega) as described previously [40]. The IκBα gene was transferred from pGEM-T Easy to pCINeo vector (Promega) by digestion with restriction enzymes followed by ligation. IκBα cloned in pGEM-T Easy vector was digested with *Eco* RI (cutting site 5' GAATTC 3') and *Spe* I (cutting site 5' ACTAGT 3'). Similarly, pCINeo was digested with *Eco* RI and *Xba* I (cutting site 5' TCTAGA 3'). As, *Spe* I and *Xba* I has compatible cohesive ends, they share a common ligation site. Thus, after digestion, digested product IκBα and digested linear fragment of pCINeo were gel eluted from agarose gel using gel elution kit (Sigma, USA). The purified digested product was ligated by NEB quick ligation kit following manufacturer's protocol. The ligation product was transformed into *E.coli* DH5α strain, and the colonies were screened by ampicillin. Further, the purified plasmids from the colonies seen on the plate were isolated and digested with *Eco* RI and *Not*I, which release digestion product of expected size. To further confirm the clone, the full length IκBα was PCR amplified using purified plasmid as a template.

2.2 Establishment of IκBα overexpressing U87MG cell line

The IκBα cloned pCINeo plasmid was purified by GenElute™ plasmid (Sigma, USA) extraction kit following manufacturer's protocol. The purified plasmid was transfected into U87MG cells by lipofectamine mediated transfection method. Here, as per the manufacturer's protocol, U87MG cells were seeded in equal number in 12 well plate, and after the cells reached 90% confluency, they were treated with lipofectamine conjugated pCINeo-IκBα plasmid. Initially, 5 µL lipofectamine and 5µg of purified plasmid were incubated in serum free media separately for 10 min, then the diluted DNA and lipofectamine were mixed together and incubated for maximum of 30 min, and added onto the cells. After 12 h, the media was replaced by normal media with 600 µg/mL G418 for selection of clonal population. The selection process was carried out until there is no cell death, with replenishing fresh media with drugs after every 3 days. Then, the RNA was isolated and the over expression of IκBα was checked to confirm the establishment of IκBα over expressing U87-IκBα cell line.

2.3 Characterization of over expression of IκBα

The over expression of IκBα in the stable cell line was assessed by the following methods-

a) Semi quantitative RT PCR: RNA was isolated from IκBα-U87MG and U87MG cells by using Trisure™ reagent (Sigma) and following the manufacturer's protocol. The cDNA of IκBα-U87MG and U87MG cells were prepared using Verso c-DNA synthesis kit (Thermo-Fischer) with the following protocol- after mixing polymerase buffer, dNTPs, RT enhancer, random hexamer, reverse transcriptase, 1 µg total RNA were mixed and required amount of water was added up to a total volume of 20 µL (as per the manufacturer's protocol). The c-DNA synthesis reaction was as follows- 42°C for 30 min then termination of the reaction at 72°C. From the synthesized c-DNA, the over expression of IκBα was detected using forward primer 5' ATGTTCCAGGCGGCCGAGCGCCC 3' and the reverse primer 5' TCATAACGTCAGACGCTGGCCTCCAAAC 3' with 30 cycle PCR with melting at 94°C, followed by another 94°C for 30 s, annealing at 56°C for 30 s and extension at 72°C for 1 min. Then, the final extension was kept for 5 min. The over expression was checked by 1% agarose gel.

b) Real time PCR: Real time PCR was performed for different cell cycle related genes using c-DNA of treated and untreated U87MG cells. For that purpose, the cells were seeded in 60 mm plate in equal number. After they reached 80% confluence, the cells were serum synchronized for 48 h. Thereafter, the serum free media was replaced with serum media. Within 2 h, the curcumin nano-conjugate were added upon the cells and incubated for 18 h. Then, the RNA was isolated and c-DNA was synthesised from 1 µg equivalent RNA. The final concentrations of primers were used as follows- β-actin (100 nM) and cyclin D1, D2, p21 and p27 (200 nM each). The primers, template (c-DNA)

and 2X SYBR green master mix and required amount of water were mixed up to a final volume of 20 µL. The real time PCR was performed for each sample in triplicate in optical 8 tube strip (0.2 mL) (MicroAmp™, Applied Biosystems, Singapore). Real time PCR was carried out in ABI 7500 Prism real time PCR machine (Applied Biosystems, USA) with standard 2 step PCR protocol. The fold change was calculated from threshold cycle (C_t) by the following formula [41] -

Fold change= $E^{\Delta\Delta C}{}_t$where, E= PCR amplification efficiency and

$\Delta\Delta C_t = \Delta C_{t,\ target} - \Delta C_{t,\ reference}$

Now, $\Delta C_{t,\ target}$= (C_t of gene of interest-C_t of housekeeping gene) target

And $\Delta C_{t,\ control}$= ((C_t of gene of interest-C_t of housekeeping gene) reference

c) Western blot analysis: The total protein from U87MG and IκBα-U87MG cells were collected by lysing the cells with RIPA buffer (Sigma) in ice followed by sonication (for 15 s) and centrifugation at 12000 x g for 30 min at 4°C. The supernatant was collected and the total protein was quantified by Lowry's method of protein estimation. Then equal amount of protein was boiled with protein loading dye (2 mL 4x dye contains 1M Tris-HCl (pH 6.8), 0.8 g SDS, 0.4 mL 100% glycerol, 160 µL 14.7 M β-mercaptoethanol, 8 mg bromophenol blue in water) and electrophoresed in 12% SDS-PAGE. Then the protein was electroblotted to PVDF membrane (pre incubated with methanol) at constant 25 V for 3 h in cooling condition. The transfer efficiency was checked by Ponceaue S staining and blocked with blocking buffer (5% BSA in TBST) for 1 h at room temperature. Then the membrane was incubated overnight at 4°C with human anti-mouse IκBα antibody (BD Pharmingen) (dilution 1:2000) and β actin (Sigma) (dilution 1:4000) in blocking buffer. Subsequently, the membrane was washed 5 times with TBST (Tris buffered saline with 0.1% Tween 20) and incubated with horseradish peroxidase (HRP) conjugated goat anti-mouse polyclonal IgG secondary antibody (Sigma) in blocking buffer (1:5000 dilution) for 2 h at room temperature. Next the membrane was washed 5 times with TBST, and probed by chemiluminiscence peroxidase substrate kit (Sigma) following manufacturer's protocol in BioradChemidoc machine.

2.4 Synthesis of curcumin nano-conjugate: The solid curcumin was dissolved in acetone at 4 mg/mL. The curcumin solution was added drop-wise to 1 mg/mL poly vinyl pyrrolidone (PVP, molecular weight 10000) solution (in water) at 75 °C to 80 °C under constant stirring up to a final concentration of 100 µg/mL of curcumin. After addition of curcumin, stirring was continued for 2-3 min, the solution was sonicated in probe sonicator (Hielscher, Germany) with 1 min pulse at 30% amplitude and 0.5 cycle for 5 min at room temperature with intermittent cooling. Then, the solution was centrifuged for 5000 x g for 5 min at 4 °C to pellet down the larger particles. The supernatant was further centrifuged at 12000xg for 10 min to collect the curcumin nanoparticles (NPs). The pellet was dissolved in Milli-Q water, and further probe sonicated to disperse the curcumin NPs. For its application upon cells, the process was carried out in aseptic condition. After synthesis of curcumin NPs, 0.01% (w/v) poly-L-lysine (PLL, Sigma, USA) was added to the curcumin NPs solution to apply positive charge to the NPs, then BSA was added at 100 µg/mL concentration to the PLL coated curcumin NPs to stabilize it before addition.

2.5 Characterization of curcumin nano-conjugate

The synthesized curcumin NPs were characterized by following methods-

2.5.1 UV-Visible and Fluorescence spectroscopy: UV-visible spectroscopic recording was done in LS45 spectrophotometer (Perkin-Elmer, USA) and fluorescence spectroscopy in Fluorolog 3 (Horiba, Japan).

2.5.2 Transmission Electron Microscopy: The curcumin NPs were analysed by a high resolution transmission electron microscope (TEM; JEM 2100; Jeol, Peabody, MA, USA) operated at a maximum accelerating voltage of 200 keV. 7 µL of synthesized curcumin NPs were drop casted onto a carbon coated copper TEM grid for analysis, dehydrated and analysed under TEM.

2.5.3 Dynamic Light scattering study: Hydrodynamic diameter of the curcumin NPs was measured by dynamic light scattering-based analysis using a Malvern ZetasizerNano ZS (Malvern, United Kingdom). The Z average size measurement was done by He-Ne laser (633 nm) with a scattering angle 90°. The zeta potential was measured by laser Doppler micro electrophoresis technique employed by the same instrument.

2.6 Cell viability assay

Glioblastoma cell line U87MG was cultured in Dulbecco's modified Eagle's medium (DMEM) (Sigma, USA). The U87-IκBα cells were also grown in the same media with additional 300 µg/mL G418 (Sigma, USA) drug for maintaining the transfected cells. Cell viability test was carried out in 96 well plates (BD biosciences) in triplicate. 5-FU treatment was done for 48 h and curcuminnano-conjugate treatment was carried out for 24 h. 500 µg/mL 3-(4, 5-dimethylthiazol-2-yl)-2, 5-diphenyltetrazolium bromide (MTT, Himedia, India) dissolved in PBS (10 mM, pH-7.4) was added to each well. After 3 h, the media was carefully discarded, and the purple colour tetrazolium salt formed due to cellular respiration, was dissolved in 100 µL DMSO (SRL, India). The colorimetric measurement was performed in multi-well plate reader (Tecan Infinite M200 PRO, Switzerland) by recording the absorbance at 570 nm, and 650 nm for background subtraction. Thus, the cell viability was measured by following equation

$$\%\ \text{of cell viability} = \frac{(A_{570} - A_{650})_{\text{sample}}}{(A_{570} - A_{650})_{\text{control}}} \times 100$$

A_{570} represents Absorbance at 570 nm and A_{650} represents Absorbance at 650 nm.

2.7 Cell cycle analysis by flow cytometry

The effect of curcumin nano-conjugate on the cell cycle of U87MG and U87-IκBα was investigated by propidium iodide (PI) (Sigma Aldrich, USA) based flow cytometry analysis. After 24 h of treatment (at IC_{50} dose), the cells were fixed by chilled ethanol (70% v/v). The fixed cells were pelleted at 450 x g at 4 °C for 6 min and washed twice with cold PBS. The fixed cells were incubated in dark for 30 min with 50 µg/mL PI and 100 µg/mL RNaseA (Amresco, USA) and 0.1% (v/v) Triton X-100 (Sigma, USA) in PBS. Then, the 15000 cells for each sample were analysed in FACS Calibur (BD Biosciences, USA) in FL-2 channel, and the data was subsequently analysed by ModFit™.

The effect of 5-FU upon the cell cycle of U87MG and U87-IκBα cells was checked in a slightly different manner. First the cells were synchronized at G1 phase by incubating the cells for 48 h with serum free media, which was then replaced with media

containing serum along with 5-FU. Then the cells were fixed and processed for flow cytometry by above mentioned protocol.

2.8 Epi fluorescence microscopy study

The cells were incubated with curcumin nano-conjugate for 12 h, then washed with ice cold PBS twice and further stained with DAPI (Sigma, USA) and ethidium bromide (EB) (Sigma, USA) before observing under microscope at under epi-fluorescent microscope (Nikon ECLIPSE, TS100, Japan). The DAPI was excited under UV band pass filter (360/20 nm), curcumin nano-conjugate under blue band pass filter (480/15 nm) and EB under green band pass filter (535/20 nm) and observed at blue, green and red emission respectively. Also, bis-benzimide Hoescht 33342 tri-hydrochloride dye (Sigma, USA) was used for nuclear staining purpose.

2.9 Reactive oxygen species determination

Reactive oxygen species (ROS) produced by curcumin nano-conjugate inside the U87MG and U87-IκBα cells were determined by flow cytometry based DCFH-DA (Sigma Aldrich, USA) assay. After entering into the live cells, the ester bond of the DCFH-DA is cleaved by the cellular esterase into DCFH which upon oxidation, produce highly fluorescent end product. After treatment with curcumin nano-conjugate for 2 h, cells were washed with 10 mM PBS (pH-7.4) for two times, then 10 µM DCFH-DA was added along the cells along with 2 mL DMEM and incubated for 30 min in CO_2 incubator protected from light. Thereafter, the media was removed and cells were washed with PBS to wash off the residual dye and harvested by trypsin. Then the cells were pelleted and washed once with PBS for once, then immediately analysed by FACS Calibur. The fluorescence was recorded in FL1 channel with 15000 cells.

2.10 Detection of apoptotic population

To determine the apoptosis inducing effect of curcumin nano-conjugate, the following two experiments were carried out.

2.10.1 FITC-Annexin V and PI based double staining: One of the classical method of determining apoptotic population is double staining of the cells with FITC conjugated Annexin V and PI (FITC Annexin V Apoptosis Detection Kit II, BD Biosciences, USA) and detection by flow cytometry. One of the early signs of cells undergoing apoptosis is loss of integrity of plasma membrane, where phosphotidylserine (PS) flips from inner to outer part of the membrane. Calcium dependent protein Annexin V has a very high affinity to PS. By exploiting this event, cells undergoing apoptosis can be quantitatively detected following manufacturer's protocol. In brief, both U87MG and U87-IκBα cells grown in 60 mm plates were treated with curcumin nano-conjugate for 16 h. Then the floating as well as attached cell population were collected, washed with PBS, counted by Neubauer hemocytometer and then suspended in the binding buffer by following manufacturer's protocol. The cells were incubated with Annexin V antibody and PI and analysed using FACS.

2.10.2 Caspase-3 based flow cytometry analysis: Caspases (Cistenyl Aspartate specific proteases) are the specific family of protein, which plays important role in apoptosis. Caspases play different roles in various stages of apoptosis. Caspase-3 is commonly regarded as effector caspase. Thus, caspase-3 level is an important indicator of apoptosis. U87MG and U87-IκBα cells were plated in equal number (10^5 cells per plate) in 100 mm plate. Then the cells were left to become confluent upto 70% of plate surface area, and the cells were treated with curcumin nano-conjugate. After 14 h of treatment, the media was removed carefully, washed with cold PBS (10 mM, pH-7.4) and harvested with trypsin. The detached or semi attached cells were taken out with DMEM containing FBS (also trypsin was neutralized), centrifuged at 450xg for 6 min in 4°C. The cells were counted in hemocytometer and washed with cold PBS twice. Then, cells were fixed with 0.1% formaldehyde in PBS in 37°C for 10 min. After the fixing solution was removed, the cells were washed carefully with PBS to avoid losing the cells and permeabilized with 0.5% tween-20 in PBS for 10 min in room temperature with mild shaking. After 10 min, the cells were collected by centrifugation and washed with PBS for two times. As per the initial count, 20 µL of antibody/10^6 cells (as per manufacturer's instruction) were added to the samples and incubated for 30 min in room temperature in dark. Then the samples were immediately analysed by FACS with 15000 cells per experiment. The data was analysed by histogram analysis in BD Cellquest Pro™ software.

3. RESULTS AND DISCUSSION

3.1 Cloning of IκBα in pCINeo vector

IκBα gene was cloned into pCINeo vector as mentioned in materials and methods section. In brief, the IκBα gene was released from pGEM-T Easy backbone by *Eco*RI and *Spe*I digestions. The pCINeo backbone was also digested by *Eco* RI and *Xba* I. Then the digested insert and vector was ligated. The ligated product was transformed into *E. coli* and plated on agar plate with ampicillin screening. The cloning was checked by digestion with *Eco* RI and *Not* I, which generated a 970 bp fragment (Fig. 1A).

3.2 Overexpression of IκBα in U87-IκBα cells

IκBα over expressing U87-IκBα cell line was established by lipofectamine based transfection followed by G418 antibiotic selection, as mentioned in the materials and methods section. The RNA was isolated and cDNA was synthesized from U87-IκBα and untransfected U87MG cell lines. The overexpression of full length IκBα was seen after 30 cycles of PCR using gene specific primers compared to the housekeeping β-actin as loading control. Higher expression of IκBα in transfected cell line as compared to untransfected U87MG cells was observed, whereas the β-actin band intensity was unchanged (Fig. 1B).

Further, the overexpression was probed by the real time PCR using gene specific realtime PCR primers (Supplementary information Table 1). There also, almost three fold higher expression was observed by calculating the over expression from threshold cycle (C_T) by Pfaffle method (Fig. 1C).

The IκBα overexpression was also confirmed at the protein level by immunoblotting method against mouse anti-human IκBα antibody with β-actin as loading control (Fig. 1D). The HRP conjugated goat anti-mouse antibody was used as secondary antibody.

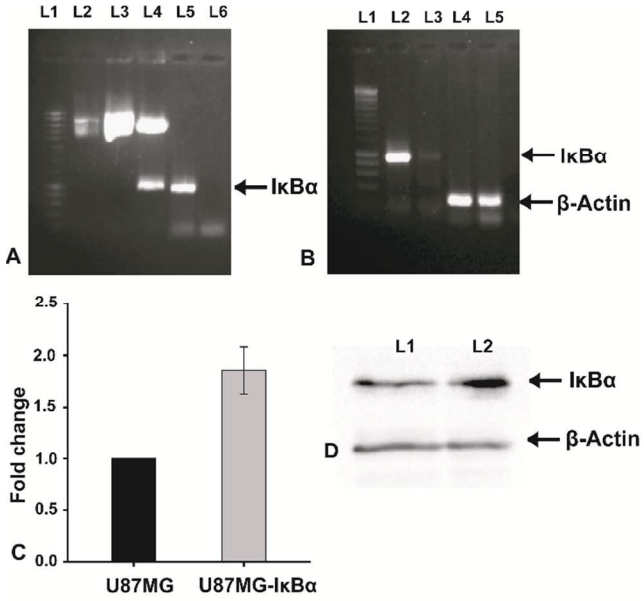

Fig. 1 Cloning and expression of cloned pCINeo-IκBα in U87MG cells. (A) Cloning of IκBα in pCINeo vector. L1: marker, L2: control pCINeo, L3: IκBα-pCINeo plasmid, L4: IκBα-pCINeo digested with EcoRI and NotI, L5: IκBα PCR product, (B) Overexpression of IκBα by semiquantitative PCR. L1: Marker, L2: IκBα expression in U87-IκBα cells, L3: Control U87MG, L4: β-actin expression in U87-IκBα cells, L5: β-actin in untransfected U87MG, (C) over expression of IκBα in transfected U87MG cells by real time PCR, (D) over expression of IκBα by Western blotting method. L1- U87MG cells alone, L2- U87-IκBα cells.

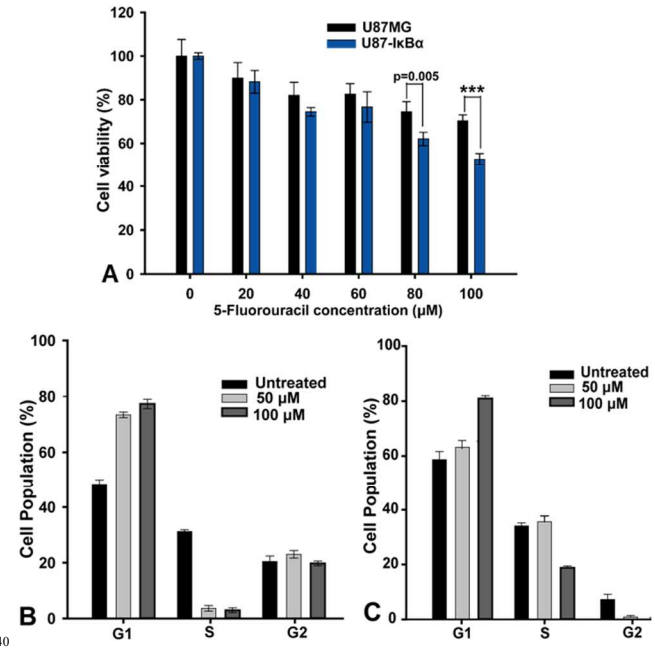

Fig. 2 Effect of 5-FU on U87MG and U87-IκBα cells. (A) Anti-cell proliferative effect of 5-FU on U87MG and U87-IκBα cells. All data are represented as Mean ± S.D. and statistical analysis was done by two way ANOVA in Sigma Plot software. Statistical significance between treated samples with significant p value (<0.05) are mentioned and p<0.001 are denoted by ***. (B) Effect of 5-Fluorouracil on the cell cycle of U87MG upon 48 h treatment by flow cytometry. (C) Effect of 5-Fluorouracil on the cell cycle of U87- IκBα upon 48 h treatment by flow cytometry.

3.3 Effect of 5-FU on U87MG and U87-IκBα cells

3.3.1 5-FU sensitization of U87MG and U87-IκBα cells: U87MG cells are known to be 5-FU resistant at admissible range. So, 5-FU was chosen to check whether IκBα over expression has any effect in sensitization of U87MG cells. After treatment with 48 h at concentration ranging from 0 μM to 100 μM, the MTT based anti-cell proliferative assay showed that, U87-IκBα cells were more sensitive towards 5-FU than U87MG cells (Fig. 2A), at longer time scale (72 h) also, the same trend of sensitization was observable (Fig. S4) which unambiguously indicated that IκBα played important role in sensitization of U87MG cells towards 5-FU.

3.3.2 Effect of 5-FU on cell cycle: The effect on cell cycle was studied by PI mediated cell cycle analysis with dose dependent manner in 48 h treatment. From the histogram analysis of each phase of cell cycle using ModFit™ software, it was evident that 5-FU has differential effect on U87MG cells and U87-IκBα cells with almost no sub G0 population in both types of cells. But with increase of 5-FU concentration, U87MG cells showed higher number of cells in G1 phase as compared to untreated U87MG cells (Fig. 2B).

But, interestingly, U87-IκBα cells showed higher number of cells in G1 and S phase with diminishing G2 phase at 50 μM of 5-FU. But at 100 μM 5-FU concentration, cells showed significant G1 phase arrest with reduced number of cells at S phase and G2 phase (Fig. 2C). The result indicated that the overexpression of IκBα changes the cellular response towards 5-FU with its increasing concentrations.

3.4 Synthesis and Characterization of curcumin nano-conjugate

Water soluble curcumin NPs were synthesized by solvent evaporation method as mentioned in earlier section. Formation of the NPs was confirmed by UV spectroscopy, fluorescence spectroscopy and TEM studies. The curcumin NPs were showing intrinsic green emission of curcumin at 550 nm when excited at 430 nm. There was no significant difference in its emission after addition of the poly-L-lysine (PLL) and BSA, which served as a surface stabilizing agent for the NPs (Fig. 3A). It is worth mentioning that PLL and BSA together played important role in terms of providing positive charge as well as stabilization of the nano-conjugate (Fig. S2). The surface charge of nanoparticle between -10 mV to +10 mV is ideal for cellular internalization [46, 47]. The TEM image of the curcumin nano-conjugate revealed that most of the NPs were spherical in nature and the average particle size was found to be 225±40 nm. The particle size distribution obtained from TEM image is calculated by Image J software and shown in supplementary information (Fig. S1). To substantiate the above results hydrodynamic diameter was determined by dynamic light scattering analysis (DLS). The hydrodynamic diameter or Z-average diameter and zeta potential of the NPs were found to be 267±20 nm and 10.6±3.5 mV respectively, which indicates that size and the surface properties of the NPs are suitable for the cellular uptake [48, 49]. The representative images of TEM and hydrodynamic diameter of the protein loaded particle are shown below (Fig. 3B and 3C).

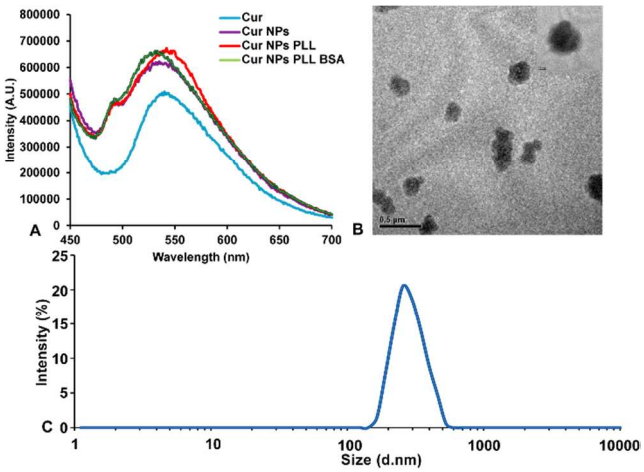

Fig. 3 Characterization of curcumin nano-conjugate by (A) emission spectra showing the emission of curcumin at 550 nm when excited at 430 nm. (B) TEM image of the curcumin nano-conjugate. (C) DLS data showing the hydrodynamic diameter of the curcumin nano-conjugate (267 nm).

3.5 Effect of curcumin nano-conjugate on the cells

3.5.1 Cell viability assay: The impact of IκBα loaded curcumin NPs was tested on U87MG cells along with curcumin nano-conjugate to elucidate the effect of curcumin NPs alone as BSA is commonly regarded to be nontoxic to the cells. Cells were treated with curcumin nano-conjugate, ranging from 1.87 µg/mL (containing 60 ng/mL of BSA) to 7.5 µg/mL (containing 235 ng/mL of BSA) for 24 h. Thus, the effect of various concentrations of curcumin nano-conjugate were tested on both U87MG and U87-IκBα cell lines (Fig. 4A). The higher efficacy was found in U87-IκBα cells, which indicated the role of IκBα towards sensitization of U87MG to the curcumin nano-conjugate. Only curcumin NPs were found to have insignificant cytotoxicity (Fig. S5).

3.5.2 Effect of curcumin nano-conjugate on cell cycle: The effect of curcumin nano-conjugate on cell cycle was studied following the result obtained by cell viability assay. The U87-IκBα cells were treated with curcumin nano-conjugate for 24 h, and stained with PI analysed by flow cytometry method with 15000 cells for each sample. Higher number of cells was found in sub G0 population of curcumin nano-conjugate treated IκBα overexpressing U87MG cells as compared to ordinary U87MG cells. Also, for curcumin nano-conjugate treated IκBα overexpressing cells, higher number of cells were found in the G1 phase with a lower number of cells in S and G2 phase, as compared to untreated overexpressing cells, treated and untreated ordinary U87MG cells. Thus, the possibility of higher amount of apoptosis of curcumin nano-conjugate treated U87-IκBα cells emerge from the flow cytometry analysis (Fig. 4B).

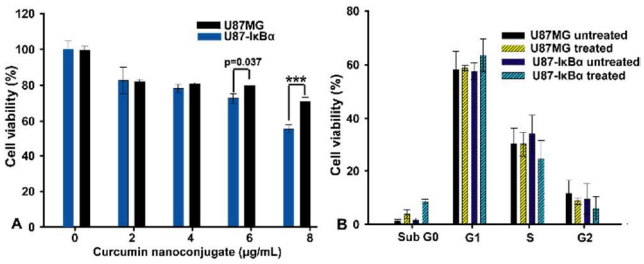

Fig. 4 Effect of curcumin nano-conjugate on U87MG and U87-IκBα cells. (A) Anti-cell proliferative effect of curcumin nano-conjugate on U87-IκBα and U87MG cells. (B) Cell cycle analysis of U87MG and U87-IκBα cells treated with curcumin nano-conjugate for 24 h. All data are represented as mean ± S.D. of three individual experiments and the statistical analysis was done by two way ANOVA in Sigma Plot software. Statistical significance between treated samples with significant p value (<0.05) are mentioned and p<0.001 are denoted by ***.

3.5.3 Gene expression analysis: The expressions of cell cycle related genes such as, cyclin D1, cyclin D2, p27 and p21 were checked to establish the underlying molecular events. Both curcumin and IκBα have been found to modulate the expression of cyclin D1 via inhibition of NFκB [42, 43]. The expression of cyclin D1 was found to be downregulated in curcumin nano-conjugate treated U87MG cells as compared to the untreated cells, which led to G1 phase arrest (Fig. 5A). Further, untreated U87- IκBα cells were found to express even lower level of cyclin D1 as a result of IκBα overexpression, which might lead to inhibition of NFκB as compared to U87MG cells (both treated and untreated). Further, the curcumin nano-conjugate treated cells showed low cyclin D1 expression, although not significant when compared to untreated cells (Fig. 5A). Cyclin D2 is another D type cyclin critical for G1 to S progression of cell cycle. There is no conclusive report stating that curcumin modulates the expression of cyclin D2 in U87MG cells, although, there is report of activation of cyclin D2 by NFκB in T cells and resting fibroblast [44]. Here, upon treatment with curcumin nano-conjugate, more than 4 fold over expression was observed for cyclin D2 in treated ordinary U87MG cells, which indicated that U87MG cells were undergoing proliferation and survival upon treatment, thus leading to higher expression of cyclin D2. But surprisingly, in U87- IκBα cells, the cyclin D2 expression level was found to be quite less (almost two fold) as compared to untreated ordinary U87MG cells. Upon treatment with curcumin nano-conjugate, the cyclin D2 was found to be significantly low, which indicated the there was a synergistic effect of both curcumin and IκBα on the curcumin NP mediated sensitization (Fig. 5B).

The role of p21 and p27 was also determined in the TNF-α mediated inhibition of human glioma cell proliferation [45]. The role of NFκB and curcumin mediated upregulation of p21 and p27 has also been reported [46, 47] at the protein level. Here the expression level of p27 (Fig. 5C) and p21 (Fig. 5D) has been measured upon treatment with curcumin nano-conjugate. The p27 expression was found to be higher in treated U87MG cells as compared to the untreated cells. For U87- IκBα cells, p27 expression was found to be higher in untreated cells as compared to the U87MG cells. In treated cells, the p27 expression was found to be significantly higher (almost three fold as compared to untreated U87MG cells and almost two fold as compared to treated U87MG and untreated U87- IκBα cells). Similarly, p21 was also found to be differentially over-expressed for both kinds of treated cells as compared to their corresponding untreated cells (Fig. 5D). The results indicated that the cell cycle arrest in G1 to S phase transition leading to apoptosis [27] is responsible for curcumin nano-conjugate mediated sensitization of IκBα over expressing glioma cells, which was found to be much higher as compared to the glioma cells.

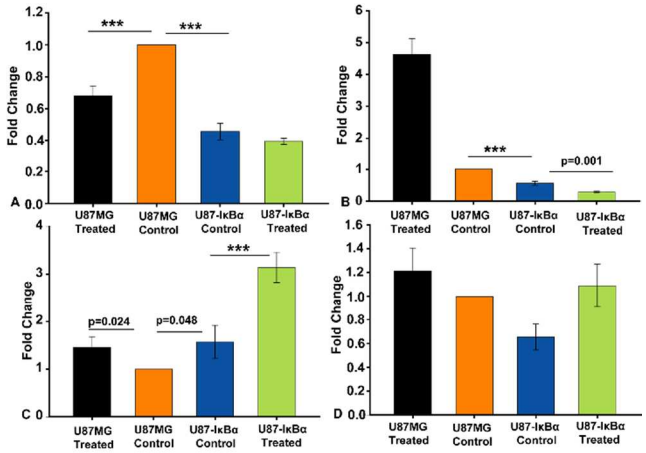

Fig. 5 Real time PCR analysis of cell cycle related genes upon treatment with curcumin nano-conjugate (A) Cyclin D1, (B) Cyclin D2 (C) p27 and (D) p21. All data are represented as mean ± S.D. and the statistical analysis was done by Rank sum test followed by Student's t test in Sigma plot software. Statistical significance between untreated control and treated samples were denoted by mentioning p value above the results or by mentioning *** when p<0.001.

3.5.4 Microscopic analysis: The microscopic analysis was carried out on both types of cells upon treatment with curcumin nano-conjugate for 12 h, and stained with DAPI and ethidium bromide (EB). DAPI is a nuclear staining dye and EB only enters through the membrane compromised cells. The goal of the experiment was to identify the live and dead cells upon treatment with curcumin nano-conjugate. Higher number of EB positive cells, which is membrane compromised, was found in IκBα overexpressing U87MG cells as compared to untransfected U87MG cells, which indicated that curcumin played pro-apoptotic function in both types of U87MG cells, but more prominent in U87-IκBα cells (Fig. 6A-H). Further, the cells were stained with another nuclear staining dye Hoescht 33342 that readily enters the cell and bind with DNA. BSA loaded curcumin nano-conjugate was also added to the cells and the interaction of the curcumin nano-conjugate with the cells was shown after 3 h (Fig. S3).

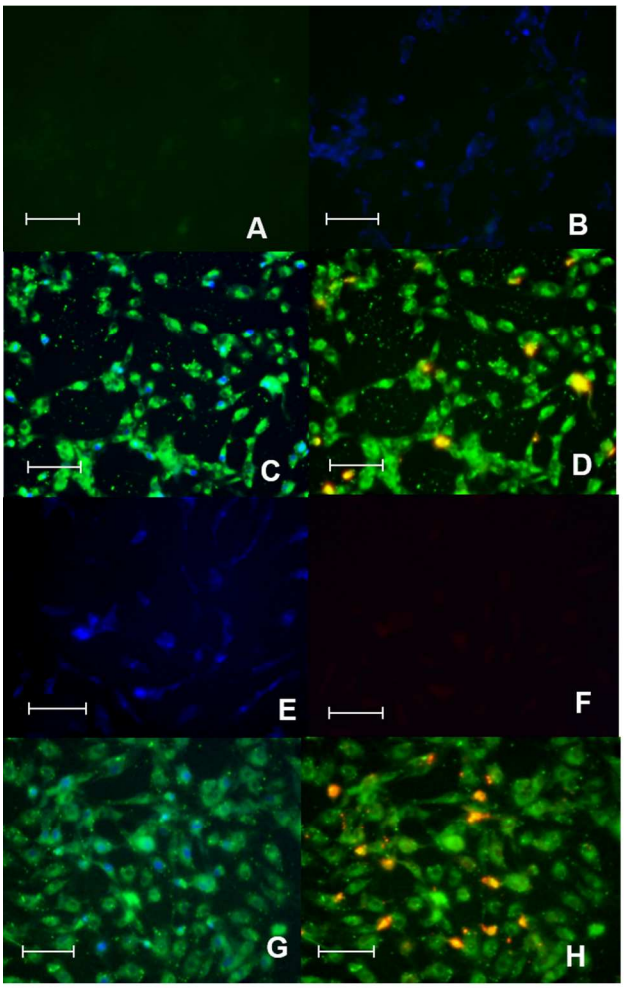

Fig. 6 Fluorescent microscopy image of curcumin nano-conjugate treated and untreated U87MG and U87-IκBα cells stained with DAPI and EB. (A) Untreated U87MG cells stained with DAPI. (B) Untreated U87MG cells stained with EB. (C) Treated U87MG cells stained with DAPI. (D) Treated U87MG cells stained with EB. (E) Untreated U87-IκBα cells stained with DAPI. (F) Untreated U87-IκBα cells stained with EB. (G) Treated U87-IκBα cells stained with DAPI. (H) Treated U87-IκBα cells stained with EB. Scale bar 100 µm.

3.5.5 ROS generation study: The generation of reactive oxygen species (ROS) influences the apoptotic event. Induction of apoptosis by protein loaded curcumin nanoparticle was studied in the previous part. Here, the effect of curcumin nano-conjugate upon IκBα overexpressing U87MG cells and ordinary U87MG have been studied by flowcytometry based DCFDA based ROS measurement. It was found that upon treatment of curcumin nano-conjugate for 3 h, U87-IκBα cells showed a higher ROS generation (Fig. 7B) as compared to U87MG (Fig. 7A), which played an important role in the curcumin nano-conjugate mediated apoptosis. Only curcumin NPs was found to induce insignificant ROS in both U87M and U87-IκBα cells (Fig. S4).

3.5.6 Detection of apoptosis: Following the trail of cell viability assay, PI based flow cytometry and microscopy analysis, the mode of cell death was confirmed by Annexin V-FITC and PI based double staining method by flow cytometry. As mentioned earlier, in the early apoptosis stage, phopsphotidyl serine (PS) of inner membrane exposed outward, which was recognised by FITC tagged Annexin V antibody. Propidium iodide was also

used to identify late apoptotic and necrotic cells. In flowcytometry, the curcuminnano-conjugate treated (for 12 h) U87- IκBα cells showed greater number of early apoptotic cells (9.12%) (Fig. 7F) as compared to the treated U87MG cells (3.17%) (Fig. 7D). This result confirmed that the mode of cells death was apoptosis.

Caspase-3 is called the executioner caspase in apoptosis event. The heightened activity of caspase-3 during the apoptosis is detected by FACS based caspase-3 assay. PE conjugated anticaspase-3 antibody is used for the purpose of studying the apoptosis event. The mode of cell death was reconfirmed by FACS based caspase-3 assay. Among BSA-curcumin NPs treated cells, U87-IκBα cells showed higher number of caspase-3 positive cells (29%) (Fig. 7J) than ordinary U87MG cells (12.7%) (Fig. 7H) after 14 h of treatment. Thus, the IκBα overexpressing cells showed more sensitivity towards BSA curcumin NPs than ordinary U87MG cells.

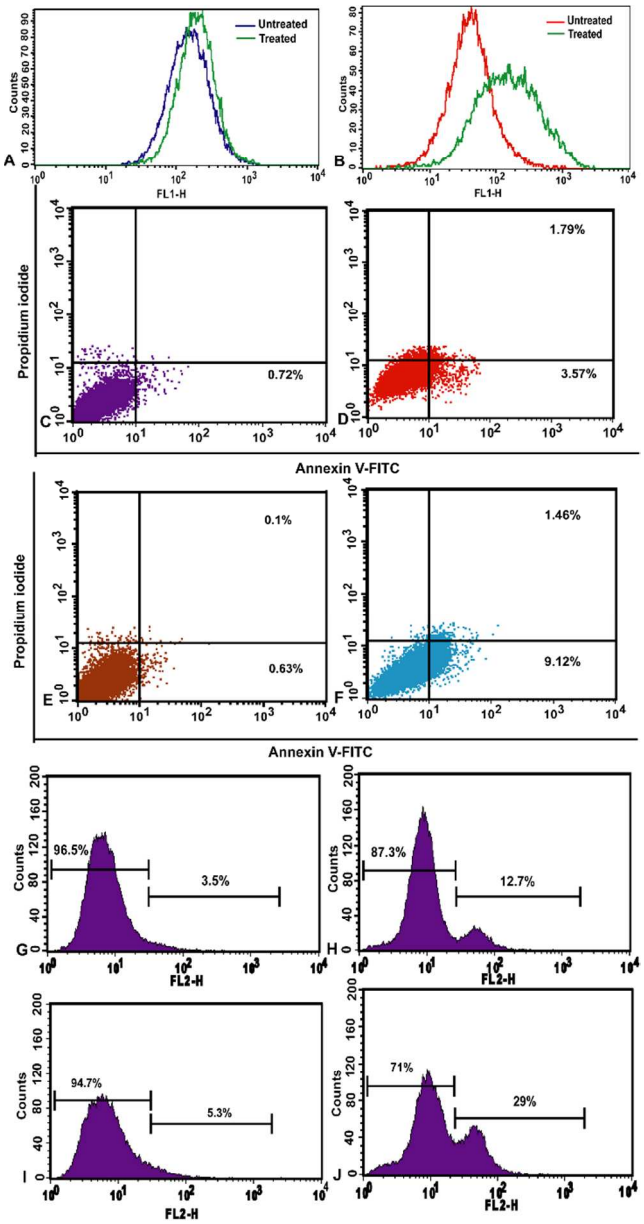

Fig. 7 Effect of curcumin nano-conjugate on U87MG and U87-IκBα cells. (A) ROS generation assay for U87MG cells. (B) ROS generation assay for U87-IκBα cells. Detection of apoptosis in U87MG cells by FITC-Annexin V and PI double staining. (C) Untreated U87MG, (D) U87MG cells treated with curcumin nano-conjugate for 12 h,(E) Untreated U87-IκBα cells and (F) U87-IκBα cells treated with curcumin nano-conjugate for 12 h. Detection of apoptosis in by Caspase-3 assay in U87MG cells upon treatment with curcumin nano-conjugate for 14 h. (G) untreated U87MG cells and (H) U87MG cells treated with curcumin nano-conjugate, (I) untreated U87-IκBα cells and (J) U87-IκBα cells treated with curcumin nano-conjugate.

3.6 Combined effect of 5-FU and curcumin nano-conjugate

The U87MG and U87-IκBα cells were treated in combination with 5-FU and curcumin nano-conjugate. This experiment was carried out in two ways- firstly, the cells were treated with different concentrations of 5-FU along with a fixed amount of curcumin nano-conjugate (5 µg/mL). It was found that in the presence of curcumin NPs, the U87-IκBα cells became more sensitized towards 5-FU (Fig. 8A). The result indicated that U87MG conferred resistance towards common anticancer drug 5-FU, even in the presence of curcumin NPs. But, IκBα overexpression sensitized U87MG significantly towards the combination therapy.

In another combination approach, the cells were treated with different concentrations of curcumin nano-conjugate with fixed concentration of 5-FU (50 µM). The cell viability decreased steadily in both the cell lines with increasing concentrations of curcumin nano-conjugate. It was found that both cell lines were equally sensitized by the combination where the effect was more in U87-IκBα cells (Fig. 8B).

The combination module had exhibited higher cytotoxicity, which could be due to action of 5-FU, curcumin and IKBα in tandem, as compared to its individual components. Earlier reports suggest that 5-FU suppressed NFκB activity and induced apoptosis in human salivary gland cancer cells by inhibiting IKKs [50, 51]. In conjunction, the presence of another inhibitor of NFκB, curcumin may also have contributed towards higher therapeutic effect on U87MG cells. In our study, curcumin nano-conjugate upon entering the cells may inhibit NFκB signalling pathways [27, 30], possibly due to known cytotoxic effect of curcumin towards cancer cells. Hence, the combination effect of 5-FU, curcumin nano-conjugate and stably expressed IκBα, which is also an inhibitor of NFκB signalling, showed heightened anti-cancer effect in U87-IκBα cells.

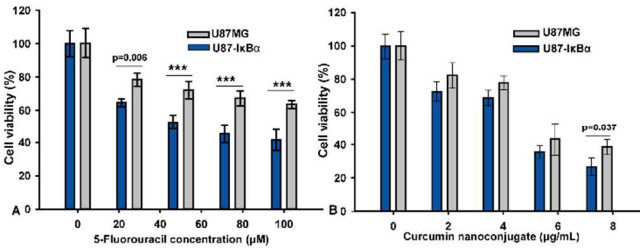

Fig. 8 Comparative study of combined effect of 5-FU and curcumin nano-conjugate on U87MG and U87-IκBα cells. (A) Effect of 5-FU in combination with curcumin nano-conjugate (5 µg/mL). (B) Effect of curcumin nano-conjugate in combination with 5-FU (50 µM). All data are represented as mean ± S.D. and the statistical analysis was done by two way ANOVA in Sigma Plot software. Statistical significance between treated samples with significant p value (<0.05) are mentioned and p<0.001 are denoted by ***.

3.7 Higher stability of IκBα

The stability of IκBα was checked by immunoblotting method. We have found the sustained expression of IκBα in U87- IκBα cells with respect to U87MG cells. At the beginning (0 min) the IκBα amount was higher in U87- IκBα cells as expected, but in the next time point (40 min) the expression level of IκBα dropped further in U87- IκBα cells than only U87MG cells. Further, at 100 min, the IκBα level in transfected U87MG cells was found to be stable, whereas there was a steady decrease in the amount of IκBα for U87MG cells. After 3h, it was found that the expression level of IκBα diminished to almost zero (Fig. 8B), whereas the amount of IκBα remained almost same for U87-IκBα cells (Fig. 8A). The result indicated that, upon treatment with curcumin nano-conjugate, the NFκB mediated survival mechanism of cells become active resulting in degradation of IκBα, although at a slower rate as curcumin is an inhibitor. But, for IκBα over expressing U87-IκBα cells, the stability of IκBα was found to have increased despite an initial drop in the amount of IκBα as compared to the U87MG cells, which indicate higher sensitization of U87- IκBα cells towards curcumin nano-conjugate.

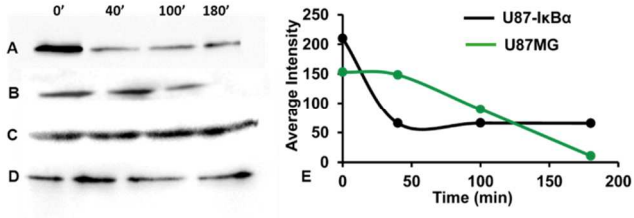

Fig. 9 Time dependent stability of IκBα in U87MG and U87-IκBα cells after treatment with curcumin nano-conjugate probed by Western blotting. (A) IκBα in U87-IκBα cells, (B) IκBα in U87MG cells, (C) β-Actin as loading control in U87-IκBα cells, (D) β-Actin as loading control in U87MG cells. (E) Change in average intensity of IκBα in U87MG and U87-IκBα cells with time.

4. CONCLUSIONS

In conclusion, IκBα was cloned into mammalian expression vector pCINeo and transfected into malignant glioblastoma cell line U87MG by lipofectamine based method. The IκBα overexpressing U87-IκBα cell line was established by screening with antibiotic G418. The overexpression of IκBα was checked by semiquantitive RT PCR, real time PCR and Western blotting with anti-IκBα antibody. The cell viability assay result indicated that U87-IκBα cells are more sensitive to 5-FU than U87MG cells. FACS based cell cycle study done by PI staining revealed that different phases of cell cycle were blocked upon treatment of 5-FU on U87MG cells and U87-IκBα cells. These results revealed that IκBα over expression sensitized the U87MG cells but they did not undergo apoptosis. Further, curcumin nano-conjugate was administered upon U87- IκBα cells and U87MG cells. It was found by cell viability assay that this module has relatively higher anti cell proliferative effect upon transfected U87MG cells. Further, the mode of cell death was microscopically examined by ethidium bromide (EB) based staining method along with intrinsic fluorescence of curcumin. A higher number of BSA-curcumin NPs treated U87-IκBα cells were found to have stained with EB, which only enters into the membrane compromised cells. Further, the effect was checked by flow cytometry assay with following experiments- PI based cell cycle analysis and determination of sub G0 population (commonly regarded as dead cells), FITC conjugated Annexin V and PI based determination of apoptotic cells and PE conjugated caspase-3 antibody based staining to determine the caspase-3 positive cell population (the cells undergoing apoptosis). Further, the expression of some cell cycle related genes was checked by real time PCR. Then the combinatorial effect of 5-FU and curcumin nano-conjugate was checked upon the U87MG and U87- IκBα cells by cell viability determination, which showed that variable concentrations of curcumin nano-conjugate with fixed concentration of 5-FU (50 μM) has higher anti-cell proliferative effect as compared to different concentrations of 5-FU with fixed (5 μg/mL) concentration of curcumin nano-conjugate. But this combinatorial effect was higher than only 5-FU. Thus, this work demonstrated that curcumin and IκBα heightened the effect of 5-FU. Further, upon treatment with curcumin nano-conjugate for different time points, the half-life of IκBα was found to have increased in IκBα transfected cells as compared to only U87MG cells, which may have an important role in sensitizing the U87MG cells towards 5-FU or curcumin NPs.The possible mode of action of the 5-FU and curcumin nano-conjugate upon U87-IκBα cells is depicted in scheme 2.

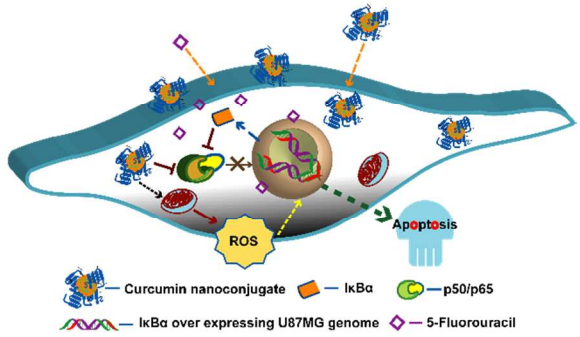

Scheme 2. Mode of action of 5-FU and curcumin nano-conjugate on U87-IκBα cells.

Notes and references

[a] *Department of Biotechnology, IIT Guwahati, Assam-781039, Guwahati, India*
[b] *Centre for Nanotechnology, IIT Guwahati, Assam-781039, Guwahati, India*
[c] *Department of Chemistry, IIT Guwahati, Assam-781039, Guwahati, India*

† Electronic Supplementary Information (ESI) available: [details of any supplementary information available should be included here]. See DOI: 10.1039/b000000x/

‡ **ACKNOWLEDGEMENTS**
The work was supported by the Department of Biotechnology (Project Nos. BT/49/NE/TBP/2010 and BT/01/NE/PS/08) and Department of Electronics and Information Technology, Government of India for financial support (No. 5(9)/2012-NANO (Vol. II)). Authors acknowledge assistance from the Central Instruments Facility (CIF) and the Centre for Nanotechnology, IIT Guwahati for TEM, FACS, Real time PCR and DLS facilities.

1. M. Mohri, H. Nitta, and J. Yamashita, *J. Neurooncol.*, 2000, **49**, 105–115.

2. D. Krex, B. Klink, C. Hartmann, A. von Deimling, T. Pietsch, M. Simon, M. Sabel, J. P. Steinbach, O. Heese, G. Reifenberger, M. Weller, G. Schackert, and for the German Glioma Network, *Brain*, 2007, **130**, 2596–2606.
3. P. Jiang, R. Mukthavavam, Y. Chao, I. Bharati, V. Fogal, S. Pastorino, X. Cong, N. Nomura, M. Gallagher, T. Abbasi, S. Vali, S. C. Pingle, M. Makale, and S. Kesari, *Journal of Translational Medicine*, 2014, **12**, 13.
4. H. Kuriyama, K. R. Lamborn, J. R. O'Fallon, N. Iturria, T. Sebo, P. L. Schaefer, B. W. Scheithauer, J. C. Buckner, N. Kuriyama, R. B. Jenkins, and M. A. Israel, *Neuro-oncology*, 2002, **4**, 179–186.
5. H. L. Pahl, *Oncogene*, 1999, **18**, 6853–6866.
6. C. Kuntzen, F. Zazzeroni, C. G. Pham, S. Papa, C. Bubici, J. R. Knabb, and G. Franzoso, *Methods Mol. Biol.*, 2007, **399**, 99–124.
7. A. S. Baldwin, *Journal of Clinical Investigation*, 2001, **107**, 3–6.
8. M. S. Hayden and S. Ghosh *Genes & Development*, 2004, **18**, 2195–2224.
9. M. S. Hayden and S. Ghosh, *Cell*, 2008, **132**, 344–362.
10. G. Ghosh, G. V. Duyne, S. Ghosh, and P. B. Sigler, *Nature*, 1995, **373**, 303–310.
11. T. Gilmore, M.-E. Gapuzan, D. Kalaitzidis, and D. Starczynowski, *Cancer Lett.*, 2002, **181**, 1–9.
12. F. Arenzana-Seisdedos, P. Turpin, M. Rodriguez, D. Thomas, R. T. Hay, J. L. Virelizier, and C. Dargemont, *J. Cell. Sci.*, 1997, **110 (Pt 3)**, 369–378.
13. P. A. Baeuerle and D. Baltimore, *Science*, 1988, **242**, 540–546.
14. B. Kaltschmidt, C. Kaltschmidt, S. P. Hehner, W. Dröge, and M. L. Schmitz, *Oncogene*, 1999, **18**, 3213–3225.
15. C. Y. Wang, M. W. Mayo, and A. S. Baldwin Jr, *Science*, 1996, **274**, 784–787.
16. B. Haefner, *Cancer Treat. Res.*, 2006, **130**, 219–245.
17. G. Madonna, C. Ullman, G. Gentilcore, G. Palmieri, and P. Ascierto, *Journal of Translational Medicine*, 2012, **10**, 53.
18. J. Adams, V. J. Palombella, E. A. Sausville, J. Johnson, A. Destree, D. D. Lazarus, J. Maas, C. S. Pien, S. Prakash, and P. J. Elliott, *Cancer Res.*, 1999, **59**, 2615–2622.
19. S. Karmakar, N. L. Banik, and S. K. Ray, *Neurochem. Res.*, 2007, **32**, 2103–2113.
20. X. Gao, D. Deeb, H. Jiang, Y. B. Liu, S. A. Dulchavsky, and S. C. Gautam, *J. Exp. Ther. Oncol.*, 2005, **5**, 39–48.
21. K. M. Dhandapani, V. B. Mahesh, and D. W. Brann, *J. Neurochem.*, 2007, **102**, 522–538.
22. A. Duvoix, R. Blasius, S. Delhalle, M. Schnekenburger, F. Morceau, E. Henry, M. Dicato, and M. Diederich, *Cancer Letters*, 2005, **223**, 181–190.
23. S. Singh and A. Khar, *Anti-Cancer Agents in Medicinal Chemistry*, 2006, **6**, 259–270.
24. A. C. Bharti, *Blood*, 2003, **101**, 1053–1062.
25. T. Choudhuri, S, Pal, T, Das and G. Sa *Journal of Biological Chemistry*, 2005, **280**, 20059–20068.
26. R. K. Srivastava, Q. Chen, I. Siddiqui, K. Sarva, and S. Shankar, *Cell Cycle*, 2007, **6**, 2953–2961.
27. S. Shishodia, H. M. Amin, R. Lai, and B. B. Aggarwal, *Biochemical Pharmacology*, 2005, **70**, 700–713.
28. S. Shishodia, P. Potdar, C. G. Gairola, and B. B. Aggarwal, *Carcinogenesis*, 2003, **24**, 1269–1279.
29. P. Anand, A. B. Kunnumakkara, R. A. Newman, and B. B. Aggarwal, *Molecular Pharmaceutics*, 2007, **4**, 807–818.
30. S. Bisht, G. Feldmann, S. Soni, R. Ravi, C. Karikar, A. Maitra, and A. Maitra, *Journal of Nanobiotechnology*, 2007, **5**, 3.
31. J. Shaikh, D. D. Ankola, V. Beniwal, D. Singh, and M. N. V. R. Kumar, *European Journal of Pharmaceutical Sciences*, 2009, **37**, 223–230.
32. M. L. Wang, W. K. Yung, M. E. Royce, D. F. Schomer, and R. L. Theriault, *Am. J. Clin. Oncol.*, 2001, **24**, 421–424.
33. S. Chockalingam and S. S. Ghosh, *PLoS ONE*, 2013, **8**, e83877.
34. K. Kurozumi, T. Tamiya, Y. Ono, S. Otsuka, H. Kambara, Y. Adachi, T. Ichikawa, H. Hamada, and T. Ohmoto, *Journal of Neuro-Oncology*, 2004, **66**, 117–127.
35. K. Kawamura, R. Bahar, H. Namba, M. Seimiya, K. Takenaga, H. Hamada, S. Sakiyama, and M. Tagawa, *Int. J. Oncol.*, 2001, **18**, 117–120.
36. K. Datta, P. Shah, T. Srivastava, S. G. Mathur, P. Chattopadhyay, and S. Sinha, *Cancer Gene Therapy*, 2004, **11**, 525–531.
37. N. M. Patel, S. Nozaki, N. H. Shortle, P. Bhat-Nakshatri, T. R. Newton, S. Rice, V. Gelfanov, S. H. Boswell, R. J. Goulet, G. W. Sledge, and H. Nakshatri, *Oncogene*, 2000, **19**, 4159–4169.
38. J. Miyakoshi and K. Yagi, *Br. J. Cancer*, 2000, **82**, 28–33.
39. R. Berger, C. Jennewein, V. Marschall, S. Karl, S. Cristofanon, L. Wagner, S. H. Vellanki, S. Hehlgans, F. Rödel, K.-M. Debatin, A. C. Ludolph, and S. Fulda, *Mol. Cancer Ther.*, 2011, **10**, 1867–1875.
40. S. Banerjee, A. K. Sahoo, A. Chattopadhyay, and S. S. Ghosh, *RSC Advances*, 2013, **3**, 14123-14131.
41. M. W. Pfaffl, *Nucleic Acids Res.*, 2001, **29**, e45.
42. D. Joyce, C. Albanese, J. Steer, M. Fu, B. Bouzahzah, and R. G. Pestell, *Cytokine Growth Factor Rev.*, 2001, **12**, 73–90.
43. A. Mukhopadhyay, S. Banerjee, L. J. Stafford, C. Xia, M. Liu, and B. B. Aggarwal, *Oncogene*, 2002, **21**, 8852–8861.
44. R. Iwanaga, E. Ozono, J. Fujisawa, M. A. Ikeda, N. Okamura, Y. Huang, and K. Ohtani, *Oncogene*, 2008, **27**, 5635–5642.
45. P. Kumar, A. Shiras, G. Das, J. C. Jagtap, V. Prasad, and P. Shastry, *Molecular Cancer*, 2007, **6**, 42.
46. B. B. Aggarwal, S. Banerjee, U. Bharadwaj, B. Sung, S. Shishodia, and G. Sethi, *Biochemical Pharmacology*, 2007, **73**, 1024–1032.
47. N. Hasima and B. B. Aggarwal, *Curr. Med. Chem.*, 2014, **21**, 1583–1594.
48. M. E. Davis, *Molecular Pharmaceutics*, 2009, **6**, 659–668.
49. A. Swami, J. Shi, S. Gadde, A. R. Votruba, N. Kolishetti, and O. C. Farokhzad, in *Multifunctional Nanoparticles for Drug Delivery Applications*, eds. S. Svenson and R. K. Prud'homme, Springer US, Boston, MA, 2012, pp. 9–29.
50. K. Aota, M. Azuma, T. Yamashita, T. Tamatani, K. Motegi, N. Ishimaru, Y. Hayashi, and M. Sato, Biochemical and Biophysical Research Communications, 2000, 273, 1168–1174.
51. M. Azuma, T. Yamashita, K. Aota, T. Tamatani, and M. Sato, Biochemical and Biophysical Research Communications, 2001, 282, 292–296.